Hu et al. Nanoscale Research Letters (2016) 11:469
DOI 10.1186/s11671-016-1693-1

Nanoscale Research Letters

NANO EXPRESS Open Access

# Ultrafine $MnO_2$ Nanowire Arrays Grown on Carbon Fibers for High-Performance Supercapacitors

Jiyu Hu[1], Feng Qian[1], Guosheng Song[2], Wenyao Li[3*] and Linlin Wang[4]

**Abstract**

Large-area ultrafine $MnO_2$ nanowire arrays (NWA) directly grew on a carbon fiber (CF, used as a substrate) by a simple electrochemical method, forming three-dimensional (3D) hierarchical heterostructures of a CF@$MnO_2$ NWA composite. As an electrode for supercapacitors, the CF@$MnO_2$ NWA composite exhibits excellent electrochemical performances including high specific capacitance (321.3 F $g^{-1}$ at 1000 mA $g^{-1}$) and good rate capability. Further, the overall capacitance retention is ~99.7 % capacitance after 3000 cycles. These outstanding electrochemical performances attribute to a large number of transport channels for the penetration of electrolyte and the transportation of ions and electrons of electrodes. The as-prepared CF@$MnO_2$ NWA composite may be a promising electrode material for high-performance supercapacitors.

**Keywords:** CF@$MnO_2$, Ultrafine nanowires, Large area, Supercapacitors

## Background

For electrochemical energy storage applications, a nanoscale solution to supercapacitors has attracted considerable attention due to their unique advantages such as faster charging/discharging rate, higher power density, much longer lifetimes, and safer operation [1–4]. Up to now, the design and synthesis of nanomaterials have promoted significant advancements in supercapacitors. One-dimensional (1D) nanostructures are believed to facilitate the electrical transport along the axial direction [5]. So far, a wide variety of nanowires, including carbonaceous materials [6, 7], transition metal oxides [8–14], conducting polymers [15, 16], and hybrid composites [17–19], have been synthesized to acquire enhanced electrochemical properties as an electrode in supercapacitors. Among them, 1D nanostructured transition metal oxides with high capacity and low cost have been a popular topic. In particular, manganese oxide (α-$MnO_2$) with high theoretical pseudocapacitance (~1370 F $g^{-1}$) has attracted intense attention due to a one-electron transfer and the complete reduction of $Mn^{IV}$ to $Mn^{III}$ as well as its environmental compatibility and earth abundance [20]. However, its poor intrinsically electrical conductivity ($10^{-5}$ to $10^{-6}$ S $cm^{-1}$) and large volume expansion during repeated cycling processes will limit its practical applications in supercapacitors [21, 22]. Thus, the design and synthesis of an electrode material based on $MnO_2$ nanowires that provides a high electrical conductivity and a reduced volume expansion are needed.

Recently, three-dimensional (3D) hierarchical heterostructures by assembling 1D $MnO_2$ nanostructures and conductive backbones, e.g., carbon materials [22, 23], nickel foam [24], and $Co_3O_4$ [25], have been demonstrated to show improved electrochemical properties in supercapacitors. In particular, a constitution within 3D heterostructures made of dense ultrafine nanowire arrays will result in high specific surface area and plentiful porosities, forming a great number of electrochemically active sites with shorter diffusion pathways for ions and electrons [26, 27]. Thus, the active materials of the electrode will improve their utilization, i.e., easily participate in reversible redox reactions with the electrolyte solution, enhancing electrochemical kinetics during the charging and discharging process [12–27]. For samples, 3D $Co_3O_4$@$MnO_2$ hierarchical nanoneedle arrays by a hydrothermal approach showed excellent electrochemical performances

* Correspondence: liwenyao314@gmail.com
[3]School of Material Engineering, Shanghai University of Engineering Science, Shanghai 201620, People's Republic of China
Full list of author information is available at the end of the article

such as high specific capacitances of 932.8 F $g^{-1}$ at a scan rate of 10 mV $s^{-1}$ as well as long-term cycling stability [25]; hierarchical CNTs@NCS@$MnO_2$ core-shell composites via a chemical polymerization coating followed by a hydrothermal process exhibited a high specific capacitance of 312.5 F $g^{-1}$ at a current density of 1 A $g^{-1}$ and a good rate capability (76.8 % retention with the charge-discharge rate increasing from 1 to 10 A $g^{-1}$) [28]. However, in the two cases, using a special template ($Co_3O_4$ nanoneedles or CNTs) with unavailable sizes can make large-scale preparation and manipulations more difficult.

Herein, using commercial carbon fibers (CF) as a substrate, large-area ultrafine $MnO_2$ nanowire arrays (NWA) directly grew on a CF, forming 3D hierarchical heterostructures of a CF@$MnO_2$ NWA composite by a simple electrochemical method. The as-fabricated electrodes by the CF@$MnO_2$ NWA composite exhibited an improved specific capacitance of 321.3 F $g^{-1}$ at 1000 mA $g^{-1}$ and an excellent cycling stability in 0.5 M $Na_2SO_4$ aqueous solution, i.e., the specific capacitance of the electrodes showing 99.7 % retention after 3000 cycles.

## Methods

### Synthesis of CF@$MnO_2$ NWA Composite

Firstly, a piece of carbon fibers (~$4 \times 1$ $cm^2$) was carefully cleaned with deionized water and absolute ethanol in sequence for several times. Secondly, the electrochemical deposition was carried out in a standard three-electrode glass cell consisting of a clean carbon fiber working electrode, a platinum plate (~$1.5 \times 1.5$ $cm^2$) counter electrode, and a saturated calomel reference electrode (SCE). $MnO_2$ nanowire arrays were electrodeposited on the carbon fibers using an Autolab electrochemical workstation (PGSTAT302N potentiostat), in which deposition conditions included a current density of 0.75 mA $cm^{-2}$, a solution at 70 ± 2 °C containing 0.1 M manganese acetate ($Mn(CH_3COO)_2$) and 0.02 M ammonium acetate ($CH_3CO_2NH_4$) with 10 % dimethyl sulfoxide (DMSO), and an electrodeposit surface area of $1 \times 1$ $cm^2$. The electrodeposition process was carried out in a water bath, in which the temperature was carefully set at 70 °C. After deposition for 20 min, the CF@$MnO_2$ NWA composite was ultrasonically washed with deionized water and absolute ethanol several times and then placed in a vacuum oven at 60 °C for 2 h. Finally, the as-prepared CF@$MnO_2$ NWA composite was annealed at 200 °C for 3 h in air. The mass of the CF@$MnO_2$ NWA composite was obtained by a weight difference before and after deposition, and the mass of active material $MnO_2$ per unit area ($1 \times 1$ $cm^2$) of the electrode is about ~1.27 mg.

### Material Characterizations

Powder X-ray diffraction (XRD; Rigaku with Cu-Kα radiation and a normal $\theta$–$2\theta$ scan) was used to characterize the phases in the collected products. Morphological observation and structural analysis of the products were carried out with a scanning electron microscope (SEM; S-4800) and a transmission electron microscopy (TEM; JEM-2100F operated at 200 kV) equipped with an energy-dispersive X-ray spectrometer (EDX). The mass of the electrode materials was weighed on an XS analytical balance (Mettler Toledo; $\delta = 0.01$ mg).

### Electrochemical Characterization

Electrochemical performances were performed on the Autolab electrochemical workstation using a three-electrode mode in a 0.5 M $Na_2SO_4$ solution. The reference electrode was a SCE, and the counter electrode was a platinum plate. Standard current-voltage curves were recorded in a potential range of −0.1 to 0.9 V.

## Results and Discussion

The phase of the as-grown products was characterized by XRD, as shown in Fig. 1a. In this pattern, two strong peaks marked with "#" are originated from the carbon fibers (substrate) and the other peaks marked with "*" can be indexed to those of the tetragonal phase of α-$MnO_2$ (JCPDS: 44-0141). No peaks associated with other crystalline forms of manganese oxide were detected in the pattern. The results indicate a high purity of $MnO_2$ material on the carbon fibers. Figure 1b, c shows a low-magnification SEM image revealing the general morphology of the product. It can be seen that the $MnO_2$ nanowires grew densely and uniformly on the surface of each carbon fiber, forming a CF@$MnO_2$ NWA composite. In fact, these dense $MnO_2$ nanowires were intersected with each other to form numerous voids or space clearances, as suggested by a high-magnification SEM image in Fig. 1d. Here, the commercial carbon fibers can also be used as a roll-to-roll media to realize mass production of the CF@$MnO_2$ NWA composite, which is expected to continuously fabricate supercapacitors in the future [29].

The TEM image and the EDX pattern of the CF@$MnO_2$ NWA composite are shown in Fig. 2. Each $MnO_2$ nanowire has a length of ~1.5 μm (Fig. 2a). Notably, individual $MnO_2$ nanowires have a diameter as fine as ~9 nm. Combining the SEM observation, the as-grown composite made of ultrafine $MnO_2$ nanowire arrays and carbon fibers has remarkable advantages for its application as an electrode in the supercapacitors. Clearly, those numerous voids or space clearances among the ultrafine nanowires can provide a large number of transport channels for the penetration of electrolyte and the transportation of ions and electrons of

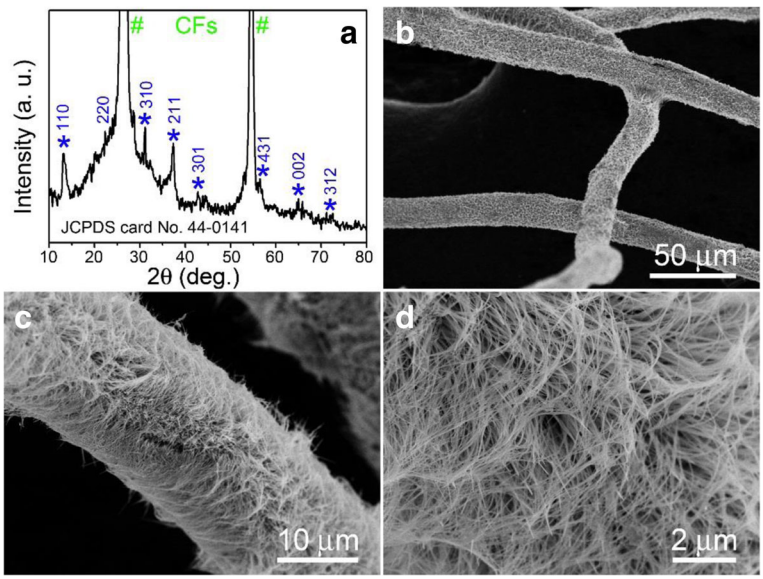


**Fig. 1** **a** XRD pattern of the as-grown $MnO_2$ nanowires on carbon fibers. **b**–**d** Different-magnification SEM images of the CF@$MnO_2$ NWA

electrodes. Furthermore, the ultrafine $MnO_2$ nanowires could greatly increase the specific surface area of the composite. These characteristics will promote the electrochemical reactions to occur on the surface and interface of the composite, finally improving the performance of the supercapacitors. The high-resolution TEM image in Fig. 2b reveals the crystalline nature of the $MnO_2$ nanowire, and the observed *d*-spacing of 0.30 nm matches well with the (110) facets of the tetragonal phase of α-$MnO_2$. The corresponding fast Fourier transform (FFT) pattern in Fig. 2c agrees with the [110] zone axis of the tetragonal phase of α-$MnO_2$. Figure 2d presents the EDX of the $MnO_2$ nanowires, which clearly indicates the presence of Mn and O elements (C signals originate from the TEM grid).

Such a composite of the ultrafine $MnO_2$ nanowire arrays directly grown on carbon fibers is used as a bind-free electrode for the supercapacitor which was examined in a 0.5 M $Na_2SO_4$ solution. Figure 3a gives cyclic voltammetry (CV) curves of the as-fabricated CF@$MnO_2$ NWA

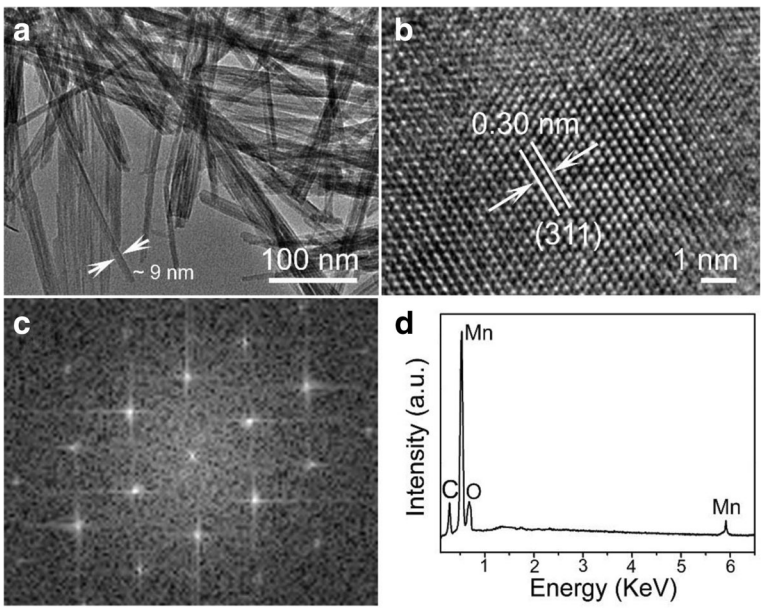


**Fig. 2** **a** TEM image of the ultrafine $MnO_2$ nanowires with a diameter of ~9 nm. **b** HRTEM image of a $MnO_2$ nanowire and **c** its corresponding FFT pattern. **d** EDX of the $MnO_2$ nanowires

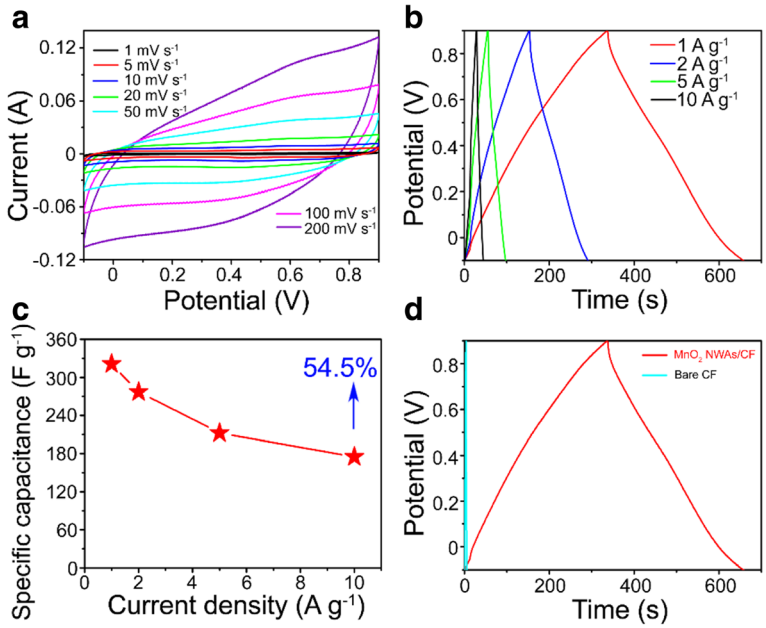


**Fig. 3** **a** CV curves of the CF@$MnO_2$ NWA electrode under different scan rates. **b** Galvanostatic charge-discharge curves of the CF@$MnO_2$ NWA electrode at different current densities. **c** Specific capacitance of the CF@$MnO_2$ NWA electrode as a function of the current density. **d** Galvanostatic charge-discharge curves of the CF@$MnO_2$ NWA and the bare CF at a current density of 1 A $g^{-1}$

electrode at different scan rates. All the curves display a nearly rectangular and symmetric characteristic, which suggests an ideal pseudocapacitive nature with fast charge and discharge processes. This could be thanks to the electrolyte coming in great numbers to the active surface of the electrode materials. Galvanostatic charge-discharge curves of the CF@$MnO_2$ NWA electrode were recorded between a potential window range of −0.1 to 0.9 V at various current densities, as shown in Fig. 3b. They appear to be an almost symmetric shape, which reflects an ideal electrochemical capacitive nature and good reversible redox reaction in the whole potential range.

Based on the discharge curves, the discharge-specific capacitance can be obtained referring to the following formula [30]:

$$C = I \cdot \Delta t / (\Delta V \cdot m) \quad (1)$$

where $C$ is the specific capacitance (F $g^{-1}$) and $I$, $\Delta t$, $\Delta V$, and $m$ are the discharge current (A), the discharge time (s) taken in the potential range, the potential windows (V), and the mass of the active materials (or the mass of the total electrode materials) (g), respectively. In line with the formula, the discharge-specific capacitances of the electrode material (CF@$MnO_2$ NWA) were calculated from the discharge curves to be 321.3, 277, 212.5, and 175 F $g^{-1}$ at the current densities of 1000, 2000, 5000, and 10,000 mA $g^{-1}$, respectively, as shown in Fig. 3c. These specific capacitances here are much higher than that in the reported works on this material with a similar composite structure [31–34].

As we know, for the supercapacitors, the rate capability is also an important aspect in their high-power applications. Figure 3c reflects the specific capacitance of the CF@$MnO_2$ NWA electrode measured at different current densities. As can be seen, the CF@$MnO_2$ NWA electrode kept 54.5 % of its specific capacitance (from 321.3 to 175 F $g^{-1}$) as the current density increased from 1000 to 10,000 mA $g^{-1}$, i.e., 10 times increase. The excellent rate capability also ascribed to the dense ultrafine space clearances inside the CF@$MnO_2$ NWA composite. Obviously, the space clearances can support numerous electrolytic accessible passageways and thus greatly help the electrolyte to penetrate into the active materials, effectively promoting the redox reactions that occurred on the surfaces and interfaces. So, even at a high rate, a considerably high specific capacitance can be obtained. In addition, these numerous passageways within the CF@$MnO_2$ NWA composite are expected to slow down the volume expansion upon a long-term cycle of repeating CV test [35]. Noticeably, the CF substrate could also affect the final capacitance of the composite electrode material. By comparing the specific capacitances of the blank CF and the CF@$MnO_2$ NWA electrode (Fig. 3d), the influence from the bare CF can be nearly negligible.

A high stability should also be required by high-performance supercapacitors. Here, a long-term cycle

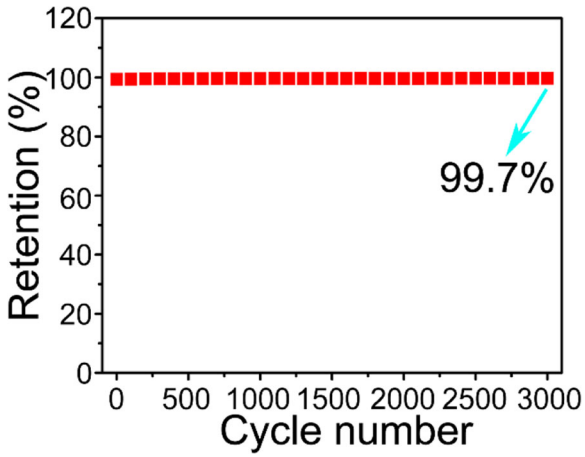


**Fig. 4** Cycling stability of the CF@$MnO_2$ NWA electrode for 3000 cycles at a scan rate of 50 mV $s^{-1}$

stability of an as-fabricated CF@$MnO_2$ NWA electrode was evaluated by repeating CV test for 3000 cycles at a scan rate of 50 mV $s^{-1}$. As shown in Fig. 4, after 3000 cycles, the capacitance retention is as high as ~99.7 %, that is, the overall loss of the capacitance is as low as ~0.3 %. In other words, this electrode represented a capacity decay rate per cycle of only 0.0001 %, which is considerably lower than those of the reported $MnO_2$-based cathodes [31–33, 36, 37]. The credit for such high stability could be given to those numerous ultrafine spaces inside the $MnO_2$ nanowire as well as the good electrical conductivity from the carbon fibers, of which the electron collection became facile and much more electrons became involved in the electrochemical reactions. It is believed that the electrode material of the CF@$MnO_2$ NWA composite can be highly competitive for a long cycle life.

## Conclusions

In summary, large-area ultrafine $MnO_2$ nanowire arrays were directly grown on carbon fiber substrates resulting in a 3D CF@$MnO_2$ NWA composite by an easy electrochemical deposition. The CF@$MnO_2$ NWA electrode demonstrates excellent electrochemical performances, i.e., ultrahigh specific capacitances of 321.3 and 175 F $g^{-1}$ at current densities of 1000 and 10,000 mA $g^{-1}$, respectively, a good rate capability, and a long cycling stability with a capacitance loss of 0.3 % after 3000 cycles. These overall fine electrochemical performances should owe to the effective electron and ion-transport pathways that originated from the distinctively microstructural characteristics of the CF@$MnO_2$ NWA composite. So, it makes the CF@$MnO_2$ NWA composite a promising electrode material for the high-performance supercapacitors.

**Acknowledgements**
This work was financially supported by the National Natural Science Foundation of China (Grant No. 51602193), and we gratefully thank the Institute of Functional Nano & Soft Materials (FUNSOM) for supporting our work.

**Authors' contributions**
JH designed and performed the experiments. JH, GS, and FQ prepared the samples and analyzed the data. JH, FQ, GS, WL, and LW participated in interpreting and analyzing the data. All authors read and wrote the manuscript. All authors read and approved the final manuscript.

**Competing interests**
The authors declare that they have no competing interests.

**Author details**
[1]No.2 High School Attached to East China Normal University, Shanghai 201203, People's Republic of China. [2]Institute of Functional Nano & Soft Materials (FUNSOM), Collaborative Innovation Center of Suzhou Nano Science and Technology, Soochow University, Suzhou, Jiangsu, People's Republic of China. [3]School of Material Engineering, Shanghai University of Engineering Science, Shanghai 201620, People's Republic of China. [4]College of Chemistry and Chemical Engineering, Shanghai University of Engineering Science, Shanghai 201620, People's Republic of China.

Received: 28 September 2016 Accepted: 15 October 2016
Published online: 20 October 2016

**References**

1. Arico AS, Bruce P, Scrosati B, Tarascon JM, Van Schalkwijk WV (2005) Nanostructured materials for advanced energy conversion and storage devices. Nat Mater 4:366
2. Chen YJ, Qu BH, Hu LL, Xu Z, Li QH, Wang TH (2013) High-performance supercapacitor and lithium-ion battery based on 3D hierarchical $NH_4F$-induced nickel cobaltate nanosheet-nanowire cluster arrays as self-supported electrodes. Nanoscale 5:9812
3. Simon P, Gogotsi Y (2008) Materials for electrochemical capacitors. Nat Mater 7:845
4. Zhu YG, Wang Y, Shi YM, Wong JI, Yang HY (2014) CoO nanoflowers woven by CNT network for high energy density flexible micro-supercapacitor. Nano Energy 3:46
5. Ma ZP, Shao GG, Fan YQ, Wang GL, Song JJ, Shen DJ (2016) Construction of hierarchical α-MnO2 nanowires@ultrathin δ-MnO2 nanosheets core-shell nanostructure with excellent cycling stability for high-power asymmetric supercapacitor electrodes. ACS Appl Mater Interfaces 8:9050
6. Yu ZN, Tetard L, Zhai L, Thomas J (2015) Supercapacitor electrode materials: nanostructures from 0 to 3 dimensions. Energy Environ Sci 8:702
7. Lee S, Ha J, Cheng H, Lee JW, Jang TS, Jung YG et al (2014) Surface-coverage-dependent cycle stability of core-shell nanostructured electrodes for use in lithium ion batteries. Adv Energy Mater 4:1300472
8. Liu W, Li X, Zhu M, He X (2015) High-performance all solid state asymmetric supercapacitor based on $Co_3O_4$ nanowires and carbon aerogel. J Power Sources 282:179
9. Cheng K, Yang F, Ye K, Zhang Y, Jiang X, Yin JL et al (2014) Highly porous $Fe_3O_4$-Fe nanowires grown on C/TiC nanofiber arrays as the high performance anode of lithium-ion batteries. J Power Sources 258:260
10. Chen R, Wang HY, Miao J, Yang H, Liu B (2015) A flexible high-performance oxygen evolution electrode with three-dimensional $NiCo_2O_4$ core-shell nanowires. Nano Energy 11:333
11. Duay J, Sherrill SA, Gui Z, Gillette E, Lee SB (2013) Self-limiting electrodeposition of hierarchical $MnO_2$ and $Mn(OH)_2$/$MnO_2$ nanofibril/nanowires: mechanism and supercapacitor properties. ACS Nano 7:1200
12. Jiao Y, Liu Y, Yin BS, Zhang SW, Qu FY, Wu X (2014) Hybrid α-$Fe_2O_3$@NiO heterostructures for flexible and high performance supercapacitor electrodes and visible light driven photocatalysts. Nano Energy 10:90
13. Yin BS, Zhang SW, Jiang H, Qu FY, Wu X (2015) Phase-controlled synthesis of polymorphic $MnO_2$ structures for electrochemical energy storage. J Mater Chem A 3:5722
14. Chen PC, Shen GZ, Shi Y, Chen HT, Zhou CW (2010) Preparation and characterization of flexible asymmetric supercapacitors based on transition-

metal-oxide nanowire/single-walled carbon nanotube hybrid thin-film electrodes. ACS Nano 4:4403
15. Tran HD, Wang Y, D'Arcy JM, Kaner RB (2008) Toward an understanding of the formation of conducting polymer nanofibers. ACS Nano 2:1841
16. Dubal DP, Lee SH, Kim JG, Kim WB, Lokhande CD (2012) Porous polypyrrole clusters prepared by electropolymerization for a high performance supercapacitor. J Mater Chem 22:3044
17. Ghosh D, Giri S, Moniruzzaman M, Basu T, Mandala M, Das CK (2014) α $MnMoO_4$/graphene hybrid composite: high energy density supercapacitor electrode material. Dalton Trans 43:11067
18. Tian W, Wang X, Zhi CY, Zhai TY, Liu DQ, Zhang C et al (2013) $Ni(OH)_2$ nanosheet@$Fe_2O_3$ nanowire hybrid composite arrays for high-performance supercapacitor electrodes. Nano Energy 2:754
19. Huang L, Chen DC, Ding Y, Wang ZL, Zeng ZZ, Liu ML (2013) Hybrid composite $Ni(OH)_2$@$NiCo_2O_4$ grown on carbon fiber paper for high-performance supercapacitors. ACS Appl Mater Interfaces 5:11159
20. Toupin M, Brousse T, Belanger D (2004) Charge storage mechanism of $MnO_2$ electrode used in aqueous electrochemical capacitor. Chem Mater 16:3184
21. Lee SW, Kim J, Chen S, Hammond PT, Shao-Horn Y (2010) Carbon nanotube/manganese oxide ultrathin film electrodes for electrochemical capacitors. ACS Nano 4:3889
22. He YM, Chen WJ, Li XD, Zhang ZX, Fu JC, Zhao CH et al (2013) Freestanding three-dimensional graphene/$MnO_2$ composite networks as ultralight and flexible supercapacitor electrodes. ACS Nano 7:174
23. Reddy ALM, Shaijumon MM, Gowda SR, Ajayan PM (2009) Coaxial $MnO_2$/carbon nanotube array electrodes for high-performance lithium batteries. Nano Lett 9:1002
24. Sun YY, Zhang WH, Li DS, Gao L, Hou CL, Zhang YH et al (2015) Direct formation of porous $MnO_2$/Ni composite foam applied for high-performance supercapacitors at mild conditions. Electrochim Acta 178:823
25. Kong DZ, Luo JS, Wang YL, Ren WN, Yu T, Luo YS et al (2014) Three-dimensional $Co_3O_4$@$MnO_2$ hierarchical nanoneedle arrays: morphology control and electrochemical energy storage. Adv Funct Mater 24:3815
26. Zhu J, Xu Z, Lu BG (2014) Ultrafine Au nanoparticles decorated $NiCo_2O_4$ nanotubes as anode material for high-performance supercapacitor and lithium-ion battery applications. Nano Energy 7:114
27. Li YH, Wang ZY, Zhang YF (2015) Ultrafine Ag/$MnO_x$ nanowire-constructed hair-like nanoarchitecture: in situ synthesis, formation mechanism and its supercapacitive property. J Alloys Compd 644:47
28. Li L, Li RM, Gai SL, Gao P, He F, Zhang ML et al (2015) Hierarchical porous CNTs@NCS@$MnO_2$ composites: rational design and high asymmetric supercapacitor performance. J Mater Chem A 3:15642
29. Gao Z, Bumgardner C, Song NN, Zhang YY, Li JJ, Li XD (2016) Cotton-textile-enabled flexible self-sustaining power packs via roll-to-roll fabrication. Nat Commun 7:11586
30. Ding SJ, Zhu T, Chen JS, Wang ZY, Yuan CL, Lou XW (2011) Controlled synthesis of hierarchical NiO nanosheet hollow spheres with enhanced supercapacitive. J Mater Chem 21:6602
31. Xia H, Hong C, Shi X, Li B, Yuan G, Yao Q et al (2015) Hierarchical heterostructures of Ag nanoparticles decorated $MnO_2$ nanowires as promising electrodes for supercapacitors. J Mater Chem A 3:1216
32. Phattharasupakun N, Wutthiprom J, Chiochan P, Suktha P, Suksomboon M, Kalasinaa S et al (2016) Turning conductive carbon nanospheres into nanosheets for high-performance supercapacitors of $MnO_2$ nanorods. Chem Commun 52:2585
33. Jiang H, Zhao T, Ma J, Yan C, Li CZ (2011) Ultrafine manganese dioxide nanowire network for high-performance supercapacitors. Chem Commun 47:1264
34. Bao LH, Zang JF, Li XD (2011) Flexible $Zn_2SnO_4$/$MnO_2$ core/shell nanocable-carbon microfiber hybrid composites for high-performance supercapacitor electrodes. Nano Lett 11:1215
35. Tao XY, Du J, Sun Y, Zhou SL, Xia Y, Huang H et al (2013) Exploring the energy storage mechanism of high performance $MnO_2$ electrochemical capacitor electrodes: an in situ atomic force microscopy study in aqueous electrolyte. Adv Funct Mater 23:4745
36. Lu XF, Wang AL, Xu H, He XJ, Tong YX, Li GR (2015) High-performance supercapacitors based on $MnO_2$ tube-in-tube arrays. J Mater Chem A 3:16560
37. Bag S, Raj CR (2016) Hierarchical three-dimensional mesoporous $MnO_2$ nanostructures for high performance aqueous asymmetric supercapacitors. J Mater Chem A 4:587